Cdc42 and actin control polarized expression of TI-VAMP-vesicles to neuronal growth cones and their fusion with the plasma membrane.

Philipp Alberts, Rachel Rudge, Theano Eirinopoulou, Lydia Danglot, Cécile Gauthier-Rouvière, Thierry Galli

Manuscript accepted for publication in Molecular Biology of the Cell (doi.10.1091/mbc.E05-07-0643)

Cdc42 and actin control polarized expression of TI-VAMP-vesicles to neuronal growth cones and their fusion with the plasma membrane

Philipp Alberts[1,2*], Rachel Rudge[1,2], Theano Eirinopoulou[3], Lydia Danglot[1,2], Cécile Gauthier-Rouvière[4], and Thierry Galli[1,2§]

[1] "Membrane Traffic in Neuronal and Epithelial Morphogenesis", INSERM Avenir Team, 75005, Paris, France

[2] Institut Jacques Monod, UMR 7592 CNRS, Universities Paris 6 and 7, Paris, France

[3] INSERM U536, Institut du Fer-à-Moulin, Paris, France

[4]"Rho GTPases, Adhesion and skeletal muscle", CRBM-CNRS FRE 2593, Montpellier, FRANCE

7618 words, 8 figures, 2 table, 3 movies.

* Present address: Department of Cell Biology, Yale University School of Medicine, P.O. Box 208002, New Haven, CT 06520

§ To whom correspondence should be addressed:

Team "Avenir" INSERM Membrane Traffic in Neuronal & Epithelial Morphogenesis

Institut Jacques Monod, UMR7592, CNRS, Universités Paris 6 & 7.

2, place Jussieu, F-75251 Paris Cedex 05, France

mailto:thierry@tgalli.net

office +33 144 278

fax +33 144 278 210

http://thierry.galli.free.fr/

Abstract

Tetanus neurotoxin Insensitive-Vesicle Associated Membrane Protein (TI-VAMP)-mediated fusion of intracellular vesicles with the plasma membrane is crucial for neurite outgrowth, a pathway not requiring synaptobrevin-dependent exocytosis. Yet, it is not known how the TI-VAMP membrane trafficking pathway is regulated or how it is coordinated with cytoskeletal dynamics within the growth cone that guide neurite outgrowth. Here, we demonstrate that TI-VAMP, but not synaptobrevin 2, concentrates in the peripheral, F-actin-rich region of the growth cones of hippocampal neurons in primary culture. Its accumulation correlates with and depends upon the presence of F-actin. Moreover, acute stimulation of actin remodeling by homophilic activation of the adhesion molecule L1 induces a site directed, actin dependent recruitment of the TI-VAMP compartment. Expression of a dominant-positive mutant of Cdc42, a key regulator of cell polarity, stimulates formation of F-actin- and TI-VAMP-rich filopodia outside the growth cone Furthermore, we report that Cdc42 activates exocytosis of pHLuorin tagged TI-VAMP in an actin-dependent manner. Collectively, our data suggest that Cdc42 and regulated assembly of the F-actin network control the accumulation and exocytosis of TI-VAMP-containing membrane vesicles in growth cones to coordinate membrane trafficking and actin remodeling during neurite outgrowth.

Introduction

One of the most striking features of neurons is their extremely elongate form, with their axons and dendrites extending frequently over tens of centimetres. Axons and dendrites elongate through specialised, highly motile growth cones. Leading the movement at the tips of the developing neurites, the growth cones extend by fusing membrane vesicles with their plasma membrane and by the constant growth and reorganisation of the cytoskeleton below this plasma membrane that pushes the leading edge forward. Although the role of cytoskeletal dynamics in the navigation of growth cones is well established (Song and Poo, 2001; da Silva and Dotti, 2002), no link has yet been found between the cytoskeleton and the membrane trafficking machinery that delivers membrane vesicles for growth.

Soluble N-ethylmaleimide sensitive factor Attachment protein Receptors (SNAREs) constitute the core machinery for membrane fusion and are involved in all of the fusion events along the biosynthetic and endocytic pathways (for review see Rothman (2002)). The membrane fusion mechanism involved in neurite outgrowth differs from the ‘classical’ synaptic core machinery inasmuch as it is unaffected by treatment with tetanus neurotoxin (TeNT), which cleaves the classical synaptic vesicle SNARE synaptobrevin 2 (Syb2) and so blocks neurotransmitter release (Osen-Sand *et al.*, 1996; Grosse *et al.*, 1999). Accordingly, the brains of Syb2 null mice develop normally up to birth (Schoch *et al.*, 2001). In contrast, a specific membrane fusion machinery may be involved in neuronal development as a mutant of the exocyst component Sec5 shows impaired neurite outgrowth but normal release of neurotransmitter in *Drosophila melanogaster* (Murthy *et al.*, 2003). We have shown that a TeNT-insensitive vesicle-associated membrane protein (TI-VAMP; also called VAMP-7), which is also a member of a subfamily of vesicular SNAREs (Filippini *et al.*,

2001; Rossi *et al.*, 2004), plays a major role in neurite outgrowth (Martinez-Arca *et al.*, 2000; Martinez-Arca *et al.*, 2001; Alberts *et al.*, 2003). However, the precise mechanism by which TI-VAMP-mediated fusion leads to growth and how it is regulated are not known.

In this paper, we set out to test the possible coordination of TI-VAMP-mediated trafficking with actin in neuronal growth cones as a way to integrate membrane traffic and cytoskeleton dynamics in neurite elongation and polarisation.

Materials and Methods

Antibodies and fluorescent reagents

Mouse monoclonal antibody to TI-VAMP (Cl 158.2) was described earlier (Muzerelle *et al.*, 2003). The polyclonal anti-GFP antibody we used was described earlier (Martinez-Arca *et al.*, 2001). Mouse monoclonal antibody against Syb2 (clone 69.1) was a generous gift from R. Jahn (Max Planck Institute, Goettingen, FRG). Mouse monoclonal antibodies against EEA1 and CD63 were from Transduction Laboratories (Becton Dickinson, Franklin Lakes, NJ, USA) and from Ancell (Bayport, MN, USA), respectively. Polyclonal anti-RFP antibody (Ab3216) was from Chemicon (Temecula, CA, USA). Affinity-purified Cy3- and Cy5-coupled goat anti-rabbit and anti-mouse immunoglobulins were from Jackson ImmunoResearch (West Grove, PA, USA). Alexa 488-coupled goat anti-rabbit and anti-mouse immunoglobulins and phalloidin coupled to Alexa 564 or 488 were from Molecular Probes (Carlsbad, CA). Fluorescent cholera toxin was a generous gift from L. Johannes (Institut Curie, Paris, France).

Plasmids

TI-VAMP-ecliptic pHLuorin (TIVAMP-epHL) was previously described (Martinez-Arca *et al.*, 2000). The mutations (F64L and S65T) required to obtain the super ecliptic variant (Sankaranarayanan *et al.*, 2000) were obtained by site-directed mutagenesis in TIVAMP-epHL. Chimeras between red fluorescent protein (mRFP) and Rho GTPases were obtained by inserting an Nhe1/BspE1 fragment from the mRFP1 (a kind gift from R. Tsien) into pEGFP-RhoAL63, pEGFP-Rac1V12 or pEGFP-Cdc42V12 (Gauthier-Rouviere *et al.*, 1998).

Cell culture and transfection

Cos7 cells were maintained in DMEM supplemented with 10% FCS. Transfection of Cos7 cells was performed using Lipofectamine 2000 according to the manufacturer's instructions. Hippocampal and cortical neurons were prepared from E18 rat brain and cultured as described (Chang and De Camilli, 2001). Transfection of cortical neurons was performed using the Amaxa Nucleofector (Amaxa GmbH, Köln, FRG) according to the manufacturer's recommendations for transfection of primary neurons.

Qualitative and quantitative immunocytochemistry

Cells in culture were fixed with 4% paraformaldehyde/ 4% sucrose and processed for immunofluorescence microscopy as described previously (Coco *et al.*, 1999). Confocal laser-scanning microscopy was performed using a SP2 confocal microscope (Leica Microsystems, Mannheim, FRG). Images were assembled using Adobe Photoshop (Adobe Systems, San Jose, CA, USA).

For comparing TI-VAMP- or Syb2-expression with F-actin content in growth cones, cells were double-labelled with monoclonal antibodies to TI-VAMP or Syb2 and Alexa564-coupled phalloidin. Images were acquired by confocal microscopy based on the actin staining and, therefore, blind for TI-VAMP- or Syb2-associated immunoreactivity. The fluorescence intensity of single confocal planes within growth cones was analysed using the region measurement function of the Metamorph software and a regression analysis was performed to statistically evaluate differences. For evaluation of TIV-, Syb2- and actin fluorescence intensity in growth cones expressing RFP or Cdc42-RFP, images were acquired from triple-labelled cells (phalloidin A488, RFP, anti-mouse Cy5) based on RFP signal, i.e. blind for the

associated TI-VAMP or actin signal, and analysis was performed as described above. Differences were evaluated statistically with the Mann-Whitney nonparametric test.

Bead-cell adhesion assay

Purification of L1Fc, production of L1 coated beads and incubation of hippocampal neurons with L1 coated beads was performed as described in (Alberts *et al.*, 2003).

Imaging and quantification of the exocytosis of TIV-pHL

TIV-pHL-expressing cells were placed in DMEM medium without riboflavine in a Ludin Chamber Type 1 (LIS, Reinach, Switzerland) and the microscope temperature was controlled using a 'Cube & Box' control system (LIS, Reinach, Switzerland). Movies were acquired on a Leica DM IRBE inverted microscope, under mercury lamp illumination with filters (GFP: excitation 475±20nm; RFP: excitation 525±45nm) piloted by a Lambda 10-2 filter wheel (AutoMate Scientific Inc. San Francisco, CA, USA), and acquired with a Cascade amplified camera (Photometrics/Roper Scientific, Evry, France). Images were acquired every two seconds with exposure times between 400 and 600 milliseconds using Metamorph (Universal Imaging, Evry France) and treated using the haze removal filtering. Quantification of the number of events was obtained by manual inspection of the movies frame by frame. 15 TIV-pHL-expressing cells were analysed for each experimental condition.

Results

We analysed the localisation of TI-VAMP in hippocampal neurons in culture by immunofluorescence microscopy and noticed striking accumulation of TI-VAMP in axonal growth cones. Moreover TI-VAMP localizes exclusively to areas that also stained intensely with fluorescent phalloidin, which binds to filamentous (F)-actin (Figure 1A) indicating that TI-VAMP localization is restricted to the so called actin rich peripheral domain of axonal growth cones (Suter *et al.*, 1998). This localisation of TI-VAMP to the F-actin-rich region of growth cones was specific because, in agreement with our earlier findings (Coco *et al.*, 1999), Syb2 was largely excluded from the growth cone periphery (Figure 1B). The immunofluorescent staining of TI-VAMP in actin-rich growth cones outlined the periphery of the growth cone, suggesting that some of the protein was associated with the plasma membrane. To confirm this conclusion, we labelled the plasma membrane of living neurons with a fluorescently labelled B subunit of cholera toxin (CtxB), which binds to GM1 (Guirland *et al.*, 2004), and costained for TI-VAMP after fixation and permeabilisation. As shown in Figure 1C, TI-VAMP (green) and CtxB (red) colocalised in the periphery of the growth cone (indicated by arrows) in regions that appear yellow in the merge, confirming the plasma membrane location of TI-VAMP and suggesting that TI-VAMP-mediated vesicle fusion with the plasma membrane might occur at the leading edge of growth cones.

We also noticed that the level of TI-VAMP staining in different growth cones was heterogeneous. Some growth cones were strongly labelled, whereas others were virtually devoid of TI-VAMP staining (Figure 2A upper panels). Since the actin cytoskeleton in growth cones is known to be highly dynamic (Suter *et al.*, 1998; Song and Poo, 2001), we hypothesised that variations in TI-VAMP staining intensity might

be related to the assembly state of the actin cytoskeleton. As shown in Figure 2A, intense labelling of F-actin in growth cones coincided with intense labelling of TI-VAMP (upper panels, marked with +), whereas growth cones that stained little for F-actin also had little labelling for TI-VAMP (upper panels, marked with -). By contrast, the F-actin content did not correlate with Syb2 labelling intensity in growth cones (Figure 2A, lower panels).

To validate these observations, we quantified the F-actin labelling intensity and compared it with the TI-VAMP or Syb2 labelling intensity in a number of growth cones (Figure 2B). Whereas the F-actin intensity correlated closely with TI-VAMP labelling (Figure 2B, R^2=0.818), we observed no correlation between F-actin and Syb2 labelling intensity in growth cones (Figure 2B, R^2=0.123). Thus, TI-VAMP expression in growth cones is positively correlated with the regulated assembly of F-actin.

We went on to test whether F-actin formation might play a role in the accumulation of TI-VAMP in growth cones by treating neurons with low concentrations of F-actin-disrupting drugs. As shown in Figure 2C, treatment of hippocampal neurons with cytochalasin B for short times led to a redistribution of F-actin into distinct, highly fluorescent foci (Figure 2C, middle right) and to a change in growth cone morphology. Interestingly, TI-VAMP also redistributed to these F-actin-rich foci (Figure 2C, middle panel left, arrows). Treatment with the cytochalasin B solvent, DMSO, alone had no effect on F-actin distribution, growth cone morphology or on the appearance of TI-VAMP in actin-rich structures (Figure 2C, upper panels). Treatment of neurons with latrunculin A disrupted the actin cytoskeleton more dramatically. Under these conditions, TI-VAMP staining became diffuse and no accumulation of the protein was observed (Figure 2C, lower panels). In contrast,

Syb2 did not redistribute to F-actin-rich foci upon treatment with cytochalasin B (Figure 2D, middle panels) nor did Syb2 staining become diffuse after incubation with latrunculin A (Figure 2D lower panels) when compared to its distribution in the control condition (DMSO treatment, Figure 2D, upper panels). Therefore, TI-VAMP accumulation in growth cones depends upon the integrity of the actin cytoskeleton, whereas the localisation of Syb2 in growth cones is not obviously affected by actin-sequestering drugs.

The correlated accumulation of F-actin and TI-VAMP in growth cones was observed in neurons grown on poly-L-Lysine in a chemically defined medium. Thus, cues leading to an assembly or disassembly of TI-VAMP and F-actin containing structures cannot be easily deduced. We have previously shown that localized homophilic engagement of the cell adhesion molecule L1 leads to a robust and specific accumulation of TI-VAMP, but not Synaptobrevin 2-containing vesicles to sites of contact (Alberts *et al.*, 2003). Furthermore, extensive remodeling of the actin cytoskeleton has been described when growth cones establish contact with a target cell (Lin and Forscher, 1993). Therefore, we made use of the previously described bead assay to mimic acutely forming L1-dependent contacts in hippocampal neurons (Alberts *et al.*, 2003). The behavior of the TI-VAMP compartment was analyzed with reference to the actin cytoskeleton after incubation of neurons with L1-coated beads. The upper panels of Figure 3A show that localized ligation of L1 on growth cones leads to a strong accumulation of both TI-VAMP and F-actin to sites of bead-cell contact. We validated these observations by quantifying the fluorescence intensity of TI-VAMP and, as a control, synaptobrevin 2 associated with actin-rich structures induced by L1 coated beads and compared to actin rich structures in growth cones not incubated with beads. As shown in figure 3B, acutely forming L1-dependent

contacts induce a local accumulation of both F-actin and TI-VAMP at contact sites when compared to control growth cones. In contrast, Synaptobrevin 2 seems to be excluded from actin rich structures forming around L1 beads as the intensity of Synaptobrevin2 staining decreases. Importantly, both the formation of F-actin rich structures and the accumulation of TI-VAMP by L1-beads were completely abolished in neurons treated with cytochalasin B (Fig 3A) or latrunculin A (our unpublished observations). Thus, L1-dependent contact formation in growth cones leads to the formation of F-actin rich structures, which are necessary for the recruitment of the TI-VAMP compartment to sites of bead-growth cone contact.

GTPases of the Rho/Rac/Cdc42 subfamily are of crucial importance in the control of cell polarity and signal-dependent actin remodelling in neurons and other cell types (Luo *et al.*, 1996; Li *et al.*, 2000; Dickson, 2002; Schwamborn and Puschel, 2004; Van Aelst and Cline, 2004). Furthermore, Rac and Cdc42 were already shown to stimulate exocytosis in mast cells (HongGeller and Cerione, 2000) and Cdc42 regulates exocytosis in adrenal chromaffin cells (Gasman *et al.*, 2004). To investigate whether these GTPases contribute to actin dependent recruitment of TI-VAMP into growth cones, we expressed dominant-positive (i.e. constitutively active) mutants of RhoA, Rac1 and Cdc42 in cortical neurons. In agreement with earlier findings in chick neurons (Brown *et al.*, 2000), we often observed enlarged growth cones and axonal shafts when we expressed dominant-positive Cdc42 mutants in cortical neurons (note the difference in magnification in Figure 4A and B). A constitutively active Cdc42 mutant, Cdc42V12, expressed as a fusion protein with red fluorescent protein (RFP), localised to the plasma membrane where it induced formation of F-actin-rich filopodia all along the axonal shaft (Figure 4B). In these neurons, TI-VAMP localized to the F-actin-rich filopodia outside the growth cone, accompanied by a large

decrease in the intensity of staining for F-actin and TI-VAMP at the leading edge of growing axons (Figure 4B). In control cells, expressing RFP alone (Figure 4A), actin and TI-VAMP remained heavily enriched in the growth cones, as in untransfected neurons (see Figs. 1-2). Despite morphological effects on the growth cones, neither the constitutively active form of Rac (RacV12) or RhoA (RhoL63), expressed as RFP fusion proteins, induced F-actin-rich filopodia outside the growth cone (Figure 4C and D) and both TI-VAMP and F-actin accumulated normally in the growth cones of cortical neurons expressing either of these mutant proteins.

To evaluate further the role of Cdc42-dependent signalling in this process, we expressed Cdc42V12-RFP and the dominant-negative Cdc42N17-RFP mutant in neurons and stained for actin and TI-VAMP or actin and Syb2. Analysis by confocal microscopy revealed that both dominant-positive and dominant-negative forms of Cdc42 reduced the apparent concentration of TI-VAMP and F-actin in growth cones (Figure 5), whereas Syb2's distribution was not obviously altered by either Cdc42 variant when compared to neurons expressing RFP alone (Figure 6). We quantified these observations by measuring the TI-VAMP- or Syb 2-associated fluorescence intensity in the F-actin rich region of the growth cone (Table 1). Dominant-positive Cdc42V12-RFP reduced the mean fluorescence intensity of staining for TI-VAMP and actin in growth cones by around 50% when compared to RFP alone, whereas dominant-negative Cdc42N17-RFP interfered with the accumulation of these proteins to a lesser, though significant extent. The intensity of staining for Syb2 in actin-rich domains of growth cones was low under all conditions tested and no statistically significant differences were detected compared with cells expressing RFP alone. Therefore, expression of dominant positive or dominant negative Cdc42 in developing neurons strongly affects TI-VAMP localization and induces a loss of

polarized expression of both TI-VAMP and actin in growth cones. In contrast, localization of Syb2 positive organelles seems to be excluded from actin rich structures in the developing neuron under all conditions tested.

We next established an assay to directly quantify TI-VAMP-dependent exocytosis and evaluate the involvement of the actin cytoskeleton and Rho GTPases in this process. To this end, we generated a pH-sensitive GFP-tagged (Miesenbock *et al.*, 1998; Sankaranarayanan *et al.*, 2000) form of TI-VAMP (TIV-pHL). First, we localized TIV-pHL in Cos7 fibroblastic cells by confocal microscopy and found that its subcellular distribution was identical to the endogenous protein with a high degree of colocalization with CD63 as already published (Martinez-Arca *et al.*, 2003a; Martinez-Arca *et al.*, 2003b) and a low degree of colocalization with EEA1, an early endosomal marker, as already shown (Coco *et al.*, 1999) (See Fig 7A). We were able to show that, as in the case of synapto-pHL, the signal emitted by plasma membrane resident TIV-pHL as measured by epifluorescence drops reversibly when living cells are incubated at pH 5 and that neutralization of intra-organelle pH with NH_4Cl results in a strong increase of signal due to the signal from intravesicular TIV-pHL (Fig 7B) (Sankaranarayanan *et al.*, 2000; Sankaranarayanan and Ryan, 2000). These results indicate that TIV-pHL fluorescence is quenched intracellularly due to the acidic pH of endosomal organelles and could therefore be used to selectively visualize surface expression of TIV-pHL. When expressed in Cos7 cells, we observed transient puffs of light by time lapse live cell microscopy that appear similar to secretory vesicle fusion events visualized using synaptopHL (Fig. 7C, see movie 1) (Miesenbock *et al.*, 1998; Sankaranarayanan and Ryan, 2000). Additionally, “worm-like” events could be observed that are likely to represent the fusion of tubules with the plasma membrane (Fig 7D and movie 1). As indicated by the arrows in Fig 7D, tubular carriers of

considerable size (distance between the two arrows in micrograph 7B “4:06” corresponds to approximately 18µM) could be observed.

As dominant-positive Cdc42V12-RFP stimulated the formation of filopodia containing F-actin and TI-VAMP in neurons, we tested the effect of expressing the same construct on the rate of exocytosis of TI-VAMP and compared it to the effect of expressing constitutively active RhoA and Rac1. Unfortunately, expression levels of TIV-pHL were insufficient for detection in neurons and therefore analysis was performed in Cos7 cells. Immunofluorescence analysis showed no obvious differences in localization or expression levels of TIVpHL when RFP or different GTPases were coexpressed (not shown). Cdc42V12-RFP had a very strong stimulatory effect on the exocytosis of TIV-pHL when compared to cells expressing RFP alone (see Movie 2 and the corresponding micrographs in Figure 8A). As shown in table 2, Cdc42V12-RFP increased by more than 10 the rate of TIV-pHL exocytosis, measured as the number of exocytic events per minute (one representative cell for each condition is presented in Figure 8A). RacV12-RFP had a moderate stimulatory effect (see table 2), whereas RhoL63-RFP was weakly inhibitory (unpublished data). Importantly, the stimulation by Cdc42V12-RFP depended upon the presence of F-actin as treatment with cytochalasin B strongly inhibited Cdc42V12-RFP-stimulated exocytosis (see Movie 3 and corresponding micrographs in Figure 8B). Thus, enhanced Cdc42 activity stimulates the exocytosis of TI-VAMP in an actin-dependent manner. Taking this data together with those presented in Figure 5, we suggest that the activity of Cdc42 and, to a lesser extent, of Rac1 control a pathway linking actin remodelling to the fusion of TI-VAMP-containing vesicles with the plasma membrane.

Discussion

In contrast to the well-characterised regulatory mechanisms of synaptic vesicle exocytosis in the mature neuron, regulatory mechanisms of membrane trafficking involved in neurite outgrowth are largely unknown. Here, we demonstrate that the dynamic assembly of the actin cytoskeleton and activity of the small GTPase Cdc42 regulates the localisation and exocytosis of TI-VAMP.

We found that TI-VAMP but not Syb2 concentrates in neuronal growth cones in an actin-dependent manner thus suggesting differential regulation of the compartmentalization of these two vesicular populations in immature neurons. This view is supported by our finding that acute local stimulation of the cell adhesion molecule L1 induces a site directed accumulation of actin and TI-VAMP, but not synaptobrevin 2 (Figure 3 and (Alberts *et al.*, 2003)). It was recently shown that the movements of GFP-Syb2 in growth cones are affected by nocodazole but not cytochalasin B (Sabo and McAllister, 2003) thus pointing to the fact that the dynamics of Syb2 depend more on microtubules than on actin. We also tested the effect of nocodazole and taxol and did not find any significant difference in the polarized concentration of TI-VAMP in growth cones (our unpublished observations). The present paper and the study by Sabo et al. (2003) therefore suggest that actin and tubulin play different functions in the compartmentalization of TI-VAMP and Syb2 in the growth cone. A likely explanation of our findings would be that F-actin targets and/or restrains the TI-VAMP, but not the Syb2, vesicles into the growth cone. Syb2 containing organelles may only be transported to the leading edge when a synapse is being generated or stabilized, as suggested by the redistribution of Syb2 to the leading edge of growth cones activated by presynaptic AMPA receptors (Schenk *et al.*, 2003).

We do not know whether the TI-VAMP vesicles are mobile within the actin-rich growth cones or if they are sequestered, thus constituting a reserve pool similar to synaptic vesicles in the mature synapse, which are tethered to an actin scaffold by synapsins and are mobilised by a phosphorylation-dependent mechanism (Sudhof, 2004). Our data indicate that TI-VAMP vesicles are directly linked to actin and rapidly mobilized to sites of growth upon signal-induced actin remodeling.TI-VAMP redistributes to actin foci after treatment with cytochalasin B or expression of Cdc42 V12 and is recruited to actin rich structures forming around L1 coated beads. Moreover actin might play a direct role in the motility and exocytosis of TI-VAMP containing vesicles towards the plasma membrane as we find TI-VAMP associated with the plasma membrane in actin rich growth cones (Fig 1) and detect an actin dependent exocytosis in Cos 7 cells expressing Cdc42 V12 (Fig 8). A role for actin in the movement of endosomes during stimulus-induced transit to the membrane has been shown recently in fibroblasts (Sandilands *et al.*, 2004). Our current working model would predict that actin dynamics control the localization and possibly exocytosis of the TI-VAMP compartment at the leading edge of growth cones and that this process provides an amplification of directed growth by polarized exocytosis.

The variability in actin and TI-VAMP expression in different growth cones suggests that signalling mechanisms exist which lead to the correlated accumulation of both markers. Indeed, Cdc42 activity might represent such a signalling mechanism, as both dominant positive as well as dominant negative Cdc42, but not Rho or Rac, interfere with the polarized expression of both actin and TI-VAMP. In comparison to CdcV12-RFP, the less dramatic effect of Cdc42N17-RFP, particularly on actin expression in growth cones, may indicate that Cdc42-independent signalling pathways are involved in the control of TI-VAMP and/or actin accumulation in growth

cones. Alternatively, expression levels of the constructs might not have been sufficient to completely abrogate Cdc42-dependent signalling.

At this point, it is unclear whether growth cones rich in actin and TI-VAMP represent fast growing axons. In fact, we used concentrations of actin depolymerizing drugs that were previously shown to have no effect on axonal outgrowth in hippocampal neurons (Rajnicek and McCaig, 1997; Bradke and Dotti, 1999; Dent and Kalil, 2001) but that were shown to abrogate attraction or repulsion of growth cones by guidance cues (Zheng *et al.*, 1996; Rajnicek and McCaig, 1997). Thus, the accumulation of the TI-VAMP-positive membrane compartment might not be necessary for efficient neurite outgrowth. Rather, it can be speculated that the actin-dependent accumulation of the TI-VAMP-compartment in the growth cone periphery may represent a mechanism to integrate actin- and membrane-dynamics to support directed growth. In this light, our finding that Cdc42 and the cell adhesion molecule L1, both of which play important roles in axonal pathfinding (Cohen *et al.*, 1998; Yuan *et al.*, 2003), can coordinate the localization of both actin and TI-VAMP in neuronal growth cones, is particularly intriguing.

We did not find any Cdc42 effectors in the several yeast two hybrid screens that we have carried out in fly embryo, human placenta (Martinez-Arca *et al.*, 2003b; Formstecher *et al.*, 2005) and human foetal brain (our unpublished observations) libraries using the Longin domain or the full cytoplasmic domain of TI-VAMP as baits. Furthermore, the recombinant cytosolic domain of TI-VAMP did not affect directly actin dynamics *in vitro* (Marie-France Carlier, Thierry Galli, unpublished observations). Therefore, the details of the molecular mechanism linking Cdc42 activation, TI-VAMP, and actin is likely to involve a complex network that will require further investigations (our unpublished observations).

In conclusion, our results are consistent with a model in which the restricted activity of Cdc42 within the growth cone mediates the polarised accumulation and exocytosis of TI-VAMP in growth cones through its regulatory action on the actin cytoskeleton. The importance of spatially restricted Cdc42 activation for directed cellular movement was demonstrated before as both dominant-positive and dominant-negative Cdc42 mutants inhibit cellular polarization and directed migration of macrophages and astrocytes (Allen *et al.*, 1998; Etienne-Manneville and Hall, 2001). We do not know the molecular cascade leading to the concentration of TI-VAMP in the growth cone and the stimulation of its exocytosis by Cdc42 in a physiological context. Yet local activation of the cell adhesion molecule L1 in neuronal growth cones induces an actin dependent recruitment of TI-VAMP-, but not Syb2-containing vesicles, to sites of contact (Figure 3 and (Alberts *et al.*, 2003). Thus it seems likely that signalling events induced by adhesion molecules like L1 activate Cdc42 leading to the actin dependent accumulation and exocytosis of TI-VAMP. The mechanism proposed here is similar to that described for phagocytosis in macrophages, another cellular process which also requires localised TI-VAMP trafficking (Braun *et al.*, 2004) upon receptor and Cdc42 activation (Hoppe and Swanson, 2004) and actin remodelling (May and Machesky, 2001). Thus, it is tempting to speculate that TI-VAMP-mediated exocytosis and actin dynamics are tightly coupled to direct the formation of cell protrusions not only in neurons and macrophages but also in other cell types, as a more general mechanism for the formation of directed cellular extensions.

Acknowledgments

The authors are grateful to Julien Cau for the mRFP-Rho GTPases constructs. This work was supported in part by grants from INSERM (Avenir Program), the European Commission (‘Signalling and Traffic’ STREP 503229), the Association pour la Recherche sur le Cancer, the Association Française contre les Myopathies, the Ministère de la Recherche (ACI-BDP), the Fondation pour la Recherche Médicale, the HFSP (RGY0027/2001-B101) and the Fondation pour la Recherche sur le Cerveau.

References

Alberts, P., Rudge, R., Hinners, I., Muzerelle, A., MartinezArca, S., Irinopoulou, T., Marthiens, V., Tooze, S., Rathjen, F., Gaspar, P., and Galli, T. (2003). Cross talk between tetanus neurotoxin-insensitive vesicle- associated membrane protein-mediated transport and L1- mediated adhesion. Mol Biol Cell *14*, 4207-4220.

Allen, W.E., Zicha, D., Ridley, A.J., and Jones, G.E. (1998). A role for Cdc42 in macrophage chemotaxis. J Cell Biol *141*, 1147-1157.

Bradke, F., and Dotti, C.G. (1999). The role of local actin instability in axon formation. Science *283*, 1931-1934.

Braun, V., Fraisier, V., Raposo, G., Hurbain, I., Sibarita, J.B., Chavrier, P., Galli, T., and Niedergang, F. (2004). TI-VAMP/VAMP7 is required for optimal phagocytosis of opsonised particles in macrophages. Embo J *23*, 4166-4176.

Brown, M.D., Cornejo, B.J., Kuhn, T.B., and Bamburg, J.R. (2000). Cdc42 stimulates neurite outgrowth and formation of growth cone filopodia and lamellipodia. J Neurobiol *43*, 352-364.

Chang, S., and De Camilli, P. (2001). Glutamate regulates actin-based motility in axonal filopodia. Nat Neurosci *4*, 787-793.

Coco, S., Raposo, G., Martinez, S., Fontaine, J.J., Takamori, S., Zahraoui, A., Jahn, R., Matteoli, M., Louvard, D., and Galli, T. (1999). Subcellular localization of tetanus neurotoxin-insensitive vesicle-associated membrane protein (VAMP)/VAMP7 in neuronal cells: Evidence for a novel membrane compartment. J.Neurosci. *19*, 9803-9812.

Cohen, N.R., Taylor, J.S., Scott, L.B., Guillery, R.W., Soriano, P., and Furley, A.J. (1998). Errors in corticospinal axon guidance in mice lacking the neural cell adhesion molecule L1. Curr Biol *8*, 26-33.

da Silva, J.S., and Dotti, C.G. (2002). Breaking the neuronal sphere: regulation of the actin cytoskeleton in neuritogenesis. Nat Rev Neurosci *3*, 694-704.

Dent, E.W., and Kalil, K. (2001). Axon branching requires interactions between dynamic microtubules and actin filaments. J Neurosci *21*, 9757-9769.

Dickson, B.J. (2002). Molecular mechanisms of axon guidance. Science *298*, 1959-1964.

Etienne-Manneville, S., and Hall, A. (2001). Integrin-mediated activation of Cdc42 controls cell polarity in migrating astrocytes through PKCzeta. Cell *106*, 489-498.

Filippini, F., Rossi, V., Galli, T., Budillon, A., D'Urso, M., and D'Esposito, M. (2001). Longins: a new evolutionary conserved VAMP family sharing a novel SNARE domain. Trends Biochem Sci *26*, 407-409.

Formstecher, E., Aresta, S., Collura, V., Hamburger, A., Meil, A., Trehin, A., Reverdy, C., Betin, V., Maire, S., Brun, C., Jacq, B., Arpin, M., Bellaiche, Y., Bellusci, S., Benaroch, P., Bornens, M., Chanet, R., Chavrier, P., Delattre, O., Doye, V., Fehon, R., Faye, G., Galli, T., Girault, J.A., Goud, B., de Gunzburg, J., Johannes, L., Junier, M.P., Mirouse, V., Mukherjee, A., Papadopoulo, D., Perez, F., Plessis, A., Rosse, C., Saule, S., Stoppa-Lyonnet, D., Vincent, A., White, M., Legrain, P., Wojcik, J., Camonis, J., and Daviet, L. (2005). Protein interaction mapping: a Drosophila case study. Genome Res *15*, 376-384.

Gasman, S., ChasserotGolaz, S., Malacombe, M., Way, M., and Bader, M.F. (2004). Regulated exocytosis in neuroendocrine cells: A role for subplasmalemmal Cdc42/N-WASP-induced actin filaments. Mol Biol Cell *15*, 520-531.

Gauthier-Rouviere, C., Vignal, E., Meriane, M., Roux, P., Montcourier, P., and Fort, P. (1998). RhoG GTPase controls a pathway that independently activates Rac1 and Cdc42Hs. Mol Biol Cell *9*, 1379-1394.

Grosse, G., Grosse, J., Tapp, R., Kuchinke, J., Gorsleben, M., Fetter, I., HohneZell, B., Gratzl, M., and Bergmann, M. (1999). SNAP-25 requirement for dendritic growth of hippocampal neurons. J.Neurosci.Res. *56*, 539-546.

Guirland, C., Suzuki, S., Kojima, M., Lu, B., and Zheng, J.Q. (2004). Lipid rafts mediate chemotropic guidance of nerve growth cones. Neuron *42*, 51-62.

HongGeller, E., and Cerione, R.A. (2000). Cdc42 and Rac stimulate exocytosis of secretory granules by activating the IP3/calcium pathway in RBL-2H3 mast cells. J Cell Biol *148*, 481-493.

Hoppe, A.D., and Swanson, J.A. (2004). Cdc42, Rac1, and Rac2 display distinct patterns of activation during phagocytosis. Mol Biol Cell *15*, 3509-3519.

Li, Z., Van Aelst, L., and Cline, H.T. (2000). Rho GTPases regulate distinct aspects of dendritic arbor growth in Xenopus central neurons in vivo. Nat Neurosci *3*, 217-225.

Lin, C.H., and Forscher, P. (1993). Cytoskeletal remodeling during growth cone-target interactions. J Cell Biol *121*, 1369-1383.

Luo, L., Hensch, T.K., Ackerman, L., Barbel, S., Jan, L.Y., and Jan, Y.N. (1996). Differential effects of the Rac GTPase on Purkinje cell axons and dendritic trunks and spines. Nature *379*, 837-840.

Martinez-Arca, S., Alberts, P., Zahraoui, A., Louvard, D., and Galli, T. (2000). Role of tetanus neurotoxin insensitive vesicle-associated membrane protein (TI-VAMP) in vesicular transport mediating neurite outgrowth. J Cell Biol *149*, 889-899.

Martinez-Arca, S., Coco, S., Mainguy, G., Schenk, U., Alberts, P., Bouille, P., Mezzina, M., Prochiantz, A., Matteoli, M., Louvard, D., and Galli, T. (2001). A common exocytotic mechanism mediates axonal and dendritic outgrowth. J Neurosci *21*, 3830-3838.

Martinez-Arca, S., Proux-Gillardeaux, V., Alberts, P., Louvard, D., and Galli, T. (2003a). Ectopic expression of syntaxin 1 in the ER redirects TI-VAMP- and cellubrevin-containing vesicles. J Cell Sci *116*, 2805-2816.

Martinez-Arca, S., Rudge, R., Vacca, M., Raposo, G., Camonis, J., Proux-Gillardeaux, V., Daviet, L., Formstecher, E., Hamburger, A., Filippini, F., D'Esposito, M., and Galli, T. (2003b). A dual mechanism controlling the localization and function of exocytic v-SNAREs. Proc Natl Acad Sci U S A *100*, 9011-9016.

May, R.C., and Machesky, L.M. (2001). Phagocytosis and the actin cytoskeleton. J Cell Sci *114*, 1061-1077.

Miesenbock, G., DeAngelis, D.A., and Rothman, J.E. (1998). Visualizing secretion and synaptic transmission with pH- sensitive green fluorescent proteins. Nature *394*, 192-195.

Murthy, M., Garza, D., Scheller, R.H., and Schwarz, T.L. (2003). Mutations in the Exocyst Component Sec5 Disrupt Neuronal Membrane Traffic, but Neurotransmitter Release Persists. Neuron *37*, 433-447.

Muzerelle, A., Alberts, P., Martinez-Arca, S., Jeannequin, O., Lafaye, P., Mazie, J.-C., Galli, T., and Gaspar, P. (2003). Tetanus neurotoxin-insensitive vesicle-associated membrane protein localizes to a presynaptic membrane compartment in selected terminal subsets of the rat brain. Neuroscience *122*, 59-75.

Osen-Sand, A., Staple, J.K., Naldi, E., Schiavo, G., Rossetto, O., Petitpierre, S., Malgaroli, A., Montecucco, C., and Catsicas, S. (1996). Common and distinct fusion proteins in axonal growth and transmitter release. J.Comp.Neurol. *367*, 222-234.

Rajnicek, A., and McCaig, C. (1997). Guidance of CNS growth cones by substratum grooves and ridges: effects of inhibitors of the cytoskeleton, calcium channels and signal transduction pathways. J Cell Sci *110 (Pt 23)*, 2915-2924.

Rossi, V., Banfield, D.K., Vacca, M., Dietrich, L.E., Ungermann, C., D'Esposito, M., Galli, T., and Filippini, F. (2004). Longins and their longin domains: regulated SNAREs and multifunctional SNARE regulators. Trends Biochem Sci *29*, 682-688.

Rothman, J.E. (2002). The machinery and principles of vesicle transport in the cell. Nature Med *8*, 1059-1062.

Sabo, S.L., and McAllister, A.K. (2003). Mobility and cycling of synaptic protein-containing vesicles in axonal growth cone filopodia. Nat Neurosci *6*, 1264-1269.

Sandilands, E., Cans, C., Fincham, V.J., Brunton, V.G., Mellor, H., Prendergast, G.C., Norman, J.C., Superti-Furga, G., and Frame, M.C. (2004). RhoB and actin polymerization coordinate Src activation with endosome-mediated delivery to the membrane. Dev Cell *7*, 855-869.

Sankaranarayanan, S., DeAngelis, D., Rothman, J.E., and Ryan, T.A. (2000). The use of pHluorins for optical measurements of presynaptic activity. Biophys J *79*, 2199-2208.

Sankaranarayanan, S., and Ryan, T.A. (2000). Real-time measurements of vesicle-SNARE recycling in synapses of the central nervous system. Nat Cell Biol *2*, 197-204.

Schenk, U., Verderio, C., Benfenati, F., and Matteoli, M. (2003). Regulated delivery of AMPA receptor subunits to the presynaptic membrane. Embo J *22*, 558-568.

Schoch, S., Deak, F., Konigstorfer, A., Mozhayeva, M., Sara, Y., Sudhof, T.C., and Kavalali, E.T. (2001). SNARE function analyzed in synaptobrevin/VAMP knockout mice. Science *294*, 1117-1122.

Schwamborn, J.C., and Puschel, A.W. (2004). The sequential activity of the GTPases Rap1B and Cdc42 determines neuronal polarity. Nat Neurosci *7*, 923-929.

Song, H., and Poo, M. (2001). The cell biology of neuronal navigation. Nat Cell Biol *3*, E81-88.

Sudhof, T.C. (2004). The synaptic vesicle cycle. Annu Rev Neurosci *27*, 509-547.

Suter, D.M., Errante, L.D., Belotserkovsky, V., and Forscher, P. (1998). The Ig superfamily cell adhesion molecule, apCAM, mediates growth cone steering by substrate-cytoskeletal coupling. J Cell Biol *141*, 227-240.

Van Aelst, L., and Cline, H.T. (2004). Rho GTPases and activity-dependent dendrite development. Curr Opin Neurobiol *14*, 297-304.

Yuan, X.B., Jin, M., Xu, X., Song, Y.Q., Wu, C.P., Poo, M.M., and Duan, S. (2003). Signalling and crosstalk of Rho GTPases in mediating axon guidance. Nat Cell Biol *5*, 38-45.

Zheng, J.Q., Wan, J.J., and Poo, M.M. (1996). Essential role of filopodia in chemotropic turning of nerve growth cone induced by a glutamate gradient. J Neurosci *16*, 1140-1149.

	RFP	Cdc42V12	Cdc42N17
TI-VAMP	**112.5 +/- 13.1** (n=19)	**55.2 +/- 11.5** (n=22) p<0.0001	**77.0 +/- 10.4** (n=21) p=0.03
Syb2	**37.3 +/- 6.3** (n=15)	**28.6 +/- 5.8** (n=13) p=0.2099	**49.8 +/- 15.5** (n=13) p=0.2002
Actin	**120.6 +/- 6.8** (n=30)	**78.3 +/- 8.0** (n=30) p=0.0005	**97.6 +/- 5.6** (n=29) p=0.012

Table 1: Mean fluorescent intensities in actin-rich domains of growth cones expressing RFP, Cdc42V12-RFP or Cdc42N17-RFP. Mean values +/- standard error (arbitrary units) of two independent experiments (n = number of neurons). P values were calculated with the Mann-Whitney nonparametric test compared with the RFP data.

	Number of cells analyzed per condition	Exocytotic active cells/total cell number (%)	Number of exocytotic events/minute
RFP	15	13	1.15+/- 0.2
Rac1 V12	15	27	3.15+/-1.9
Cdc42 V12	15	60	17+/-2.6

Table 2: Exocytotic activity of Cos 7 cells coexpressing TIVpHL and RFP, Rac1 V12 or Cdc42 V12. Exocytotic active cells represent the percentage of cells per condition showing recognizable excocytotic activity. Out of those, the mean number of exocytotic events per minute for each condition was determined.

Figure legends

Figure 1) Accumulation of TI-VAMP in the F-actin-rich region of axonal growth cones

A) Cultured hippocampal neurons grown (3 div) were costained for filamentous actin (left) and for TI-VAMP (right) and analysed by confocal microscopy (Bar=4µm).

B) A high-magnification confocal image of an axonal growth cone triple-labelled for TI-VAMP (left), Syb2 (middle) and F-actin (right) (Bar=4µm).

C) Living hippocampal neurons were labelled with fluorescent cholera toxin B (CTxB) subunit to stain the plasma membrane (middle panel and green in merge). Cells were washed, fixed and costained with a monoclonal antibody against TI-VAMP (left panel, red in merge). The TI-VAMP signal partially coincides with the plasma membrane staining by CTxB (marked by arrows, appearing as yellow in merge) (Bar=4µm).

Figure 2) TI-VAMP localisation in growth cones correlates with and depends upon actin dynamics

A) Hippocampal neurons 3 div were costained for F-actin and TI-VAMP or Syb2. Labelling intensity was analysed by confocal microscopy. In the upper panels, high labelling intensity of TI-VAMP coincides with high labelling intensity of F-actin (+), and low labelling intensity of TI-VAMP coincides with low labelling intensity of F-actin (-). Syb2-staining does not vary with the intensity of F-actin staining (lower panels; Bar=10µm).

B) Confocal images of hippocampal neurons stained for TI-VAMP or Syb2 were taken blind based on costaining for F-actin (24 images each). Labelling intensity of each marker in the entire growth cone was quantified and F-actin staining was plotted

versus the labelling intensity of associated TI-VAMP (top) or Syb2 (bottom). Whereas TI-VAMP and F-actin labelling intensities are highly correlated (Y=-6.771+1.185*X; R^2=0.818; p<0.0001), the distribution of Syb2 and F-actin labelling intensities appears random (Y=31.269+0.312*X; R^2=0.123; p=0.093).

C) Hippocampal neurons (3 div) were treated for 30min with 5µM DMSO, 5µM cytochalasin B (Cyto B) or 2.5µM latrunculin A (Latr A). Cells were analysed by confocal microscopy for expression of TI-VAMP (left) and F-actin (right). Treatment with cytochalasin B leads to a redistribution of both F-actin and TI-VAMP to highly fluorescent foci (indicated by arrows). Latrunculin A treatment disrupts the actin cytoskeleton and results in diffuse TI-VAMP staining.

D) Hippocampal neurons grown and treated as in C were analysed by confocal microscopy for expression of Syb2 (left) and F-actin (right). The distribution of Syb2 appears unaffected by the treatments (Bars=8µm).

Fig 3) Actin dependent accumulation of TI-VAMP at adhesive contacts

A) Hippocampal neurons at 3div were incubated with L1 coated beads in the presence of either DMSO or 5µM Cytochalasin B for 45 min. Cells were processed for confocal microscopy with TI-VAMP mAb (green), phalloidin (red) or L1 pAb (blue). Bead shaped structures can be recognized which are positive for TI-VAMP and F-actin and which coincide with L1-coated beads present on the growth cone shown (merge) (upper panels). Micrographs of Cytochalasin B treated cells show a number of L1 coated beads touching the extremities of the neurite (micrograph L1), but no bead shaped structures appear that are positive for TI-VAMP or F-actin (Bead diameter: 4µm).

B) Hippocampal neurons at 3div were incubated with or without L1 coated beads and stained for TI-VAMP or Synaptobrevin2 and Actin. Actin rich regions of control growth cones or growth cones in contact with beads were selected and associated fluorescence intensity for TI-VAMP or Synaptobrevin 2 and actin was quantified. Shown is the change in intensity for the different markers induced by L1 coated beads compared to control growth cones (TIV: +40.6%+/-5%, n=41, p=0.0001; Syb 2: -21.7%+/-10%, n=37, p=0.037; actin: +34%+/-7.5%, n=78, p=0.006).

Figure 4) Expression of Cdc42V12-RFP induces localisation of actin and TI-VAMP to the axonal shaft

Cortical neurons were transfected with RFP (A) or RFP-tagged Cdc42V12 (B), Rac1V12 (C) and RhoAL63 (D) and kept in culture for 5 div at low density. Cells were fixed and stained for TI-VAMP (left), F-actin (middle), and RFP (right). Confocal images of a representative growth cone are shown for each condition. Actin and TI-VAMP do not accumulate at the leading edge of the axon when Cdc42V12 is expressed in cortical neurons. Instead, filopodial structures rich in F-actin and TI-VAMP are seen (arrows). F-actin and TI-VAMP remain in the growth cones of neurons expressing Rac1V12 or RhoAL63. Note the difference in magnification (bar corresponds to 11µm for A, C, D and 18µm in B).

Figure 5) Expression of Cdc42V12-RFP and Cdc42N17-RFP interferes with accumulation of TI-VAMP in growth cones

Cortical neurons were transfected with RFP, an RFP-tagged dominant-positive form of Cdc42, Cdc42V12-RFP, or an RFP-tagged dominant-negative form, Cdc42N17-RFP, and kept in culture for five days at low density. Cells were fixed and stained for

TI-VAMP (left) or F-actin (middle). Confocal images for each condition of a representative growth cone are shown. RFP fluorescence is shown in the right-hand panels. Actin and TI-VAMP do not accumulate at the leading edge of the axon when Cdc42V12-RFP is expressed in cortical neurons and enrichment is reduced by expression of Cdc42N17-RFP. Note the enlarged axonal shaft and growth cone in neurons expressing Cdc42V12-RFP (Bar=5µm).

Figure 6) Expression of Cdc42V12-RFP and Cdc42N17-RFP does not affect Syb2 localisation

Cortical neurons were transfected and processed as described for Figure 4 and stained for Syb2, F-actin and RFP. Syb2 does not redistribute to the F-actin-rich structures induced by dominant-positive Cdc42V12-RFP but has a similar location in the central domain of growth cones under the three conditions tested (Bar=5µm).

Figure 7) Exocytosis of TI-VAMP-containing vesicles in Cos7 cells using TIV-pHL

A) Cos7 cells were transfected with cDNA encoding TIV-pHL, then fixed and labelled with a polyclonal antibody to GFP (green channel) and with a monoclonal antibody to CD63, a marker for late endosomes that colocalises with endogenous TI-VAMP, to EEA1, a marker for early endosomes. Single confocal planes are shown demonstrating a high degree of colocalisation between CD63 and TIVpHL (Upper and lower panels: Bar=10µm).

B) Live cell imaging of a Cos7 cell transfected with TIV-pHL in DMEM at pH7.0. The medium was replaced manually with a saline solution buffered to pH 5.5, changed again with saline solution buffered to pH 7.0 and then treated with 50mM NH_4Cl in

the same buffer (recordings at each condition for 2min). The epifluorescence signal emitted dropped at pH5 in a reversible manner, indicating that the signal is emitted from TIVpHL present at the cell surface, and the treatment with NH_4Cl resulted in a strong increase of fluorescence due to the contribution from TIVpHL present in intracellular organelles (Bar=15µm)

C) Cos7 cells were transfected with TIV-pHL and prepared for live imaging. Images were taken every two seconds for 9min. The images show two exocytic events just before exocytosis (01:56), an exocytotic event appearing as two bright spots (1:58) and after exocytosis and endocytosis/re-acidification and disappearance of the TIVpHL signal (2:16) (site of exocytosis is marked by two arrows).

D) A sequence of micrographs of the same cell recorded in (A) demonstrating the first appearance (4:06) and complete fusion (4:16) of a tubule with the plasma membrane. The right arrow indicates the first point of fusion with the plasma membrane (highest fluorescence intensity at time of appearance) whereas the left arrow points at the intracellular end of the tubule (C and D: Bar=10µm).

Figure 8) Cdc42V12 stimulates F-actin-dependent TIVpHL-mediated exocytosis

A) Cos7 cells were transfected with TIVpHL together with RFP or Cdc42V12-RFP and analysed for exocytosis of TIVpHL over 5min. Stills of representative cells cotransfected with RFP (top) or Cdc42V12-RFP (bottom) are shown. Transient bright TIVpHL spots, representing exocytosis, are marked by green asterisks (Bar=10µm). Cumulative plots representing the total number of exocytic events during the 5min recording time for each condition are shown on the right of each series of micrographs, the cell shapes are outlined.

B) Cos7 cells cotransfected as in (A) were analysed before and 15min after treatment with 5µM cytochalasin B. Exocytic events occurring during the sequence shown are marked with asterisks as in (A) (Bar=17µm). Corresponding cumulative plots representing the total exocytic events that occurred during the recording time (6.26min) in each condition are shown on the right of each panel, the shape of the cell recorded before and during CytB treatment is outlined in each case.

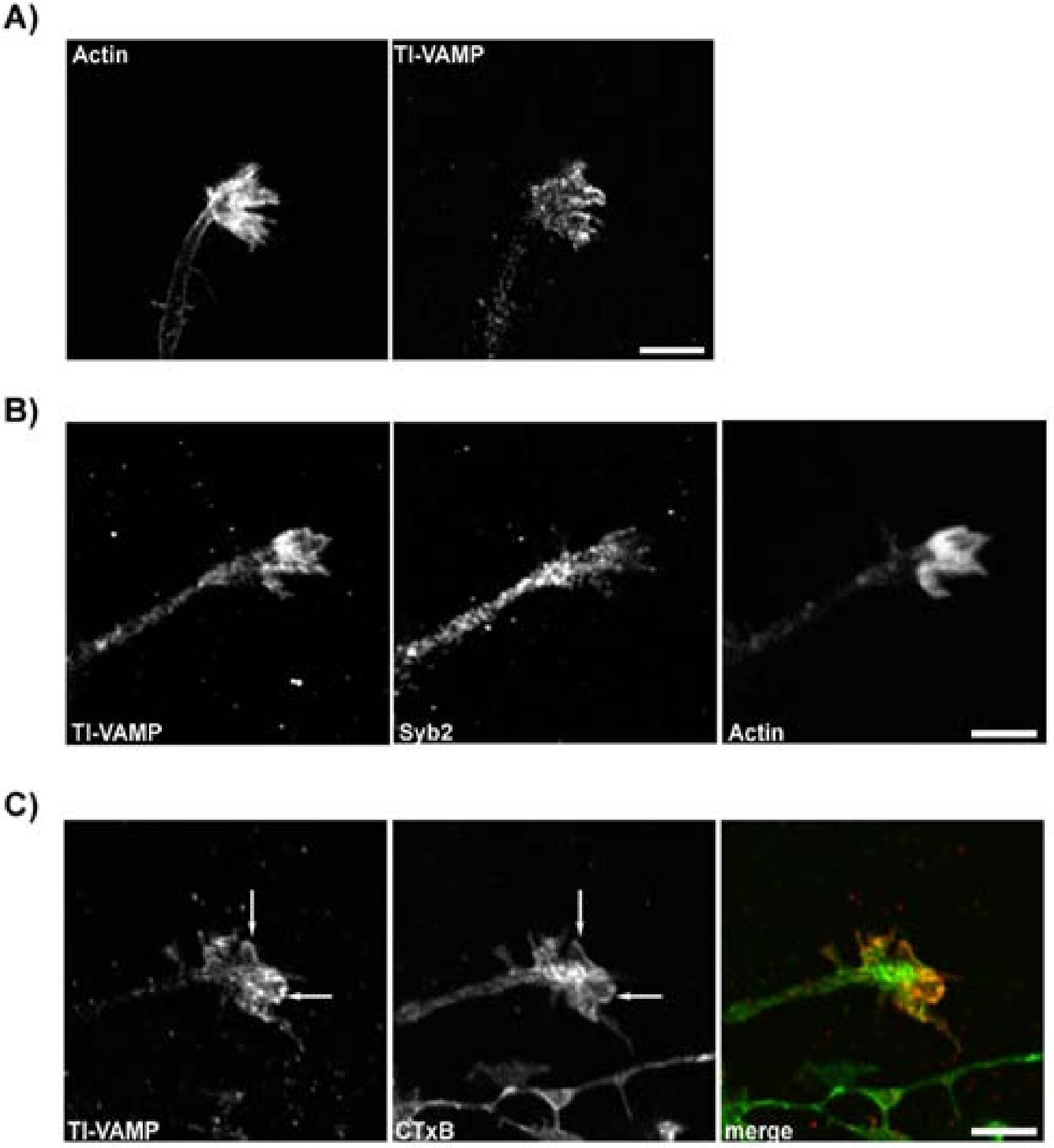
A)
Actin
TI-VAMP
B)
TI-VAMP
Syb2
Actin
C)
TI-VAMP
CTxB
merge

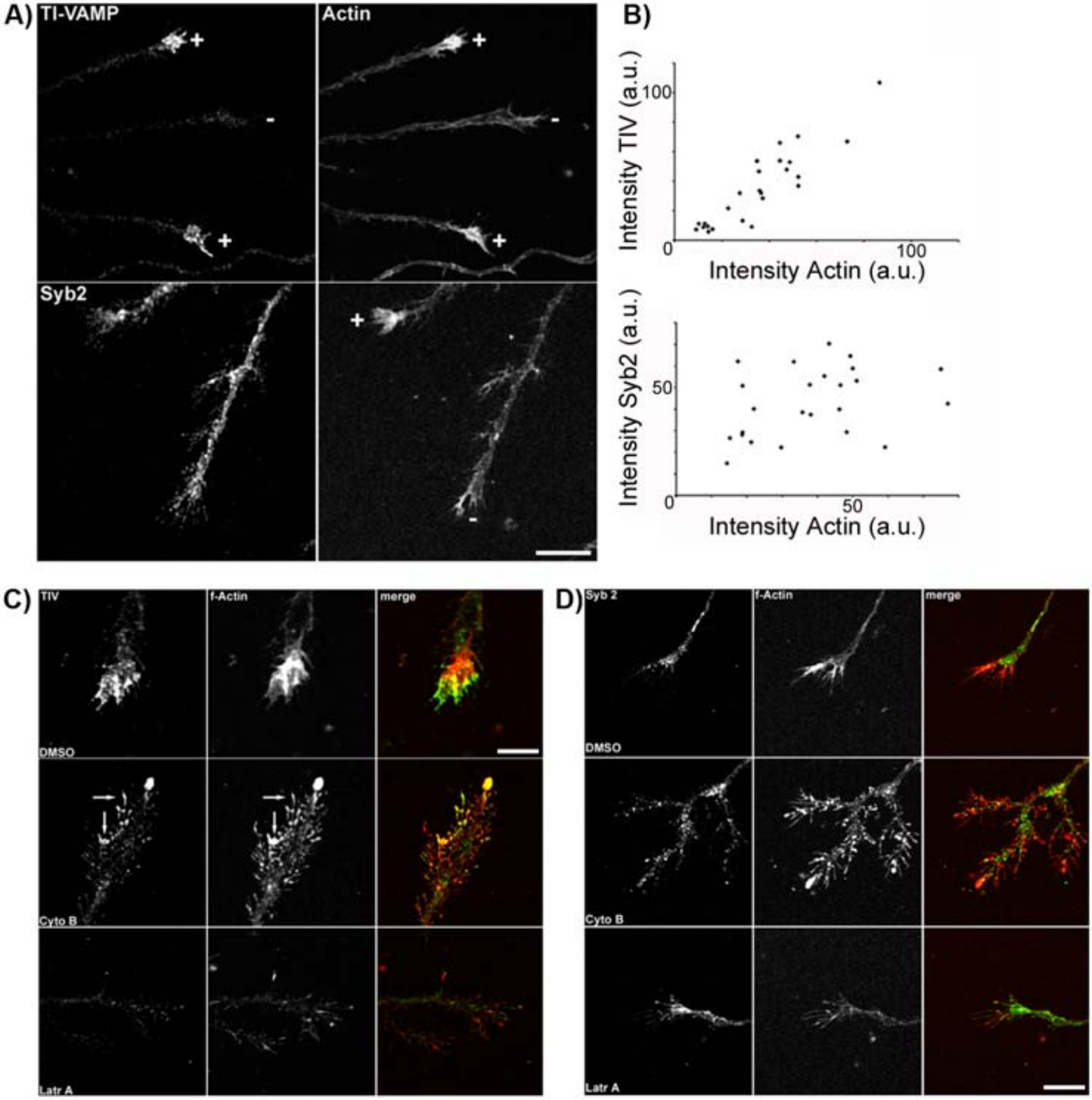
A)
TI-VAMP
Actin
Syb2
B)
Intensity TIV (a.u.)
100
0
100
Intensity Actin (a.u.)
Intensity Syb2 (a.u.)
50
0
50
Intensity Actin (a.u.)
C)
TIV
f-Actin
merge
DMSO
Cyto B
Latr A
D)
Syb 2
f-Actin
merge
DMSO
Cyto B
Latr A

A)

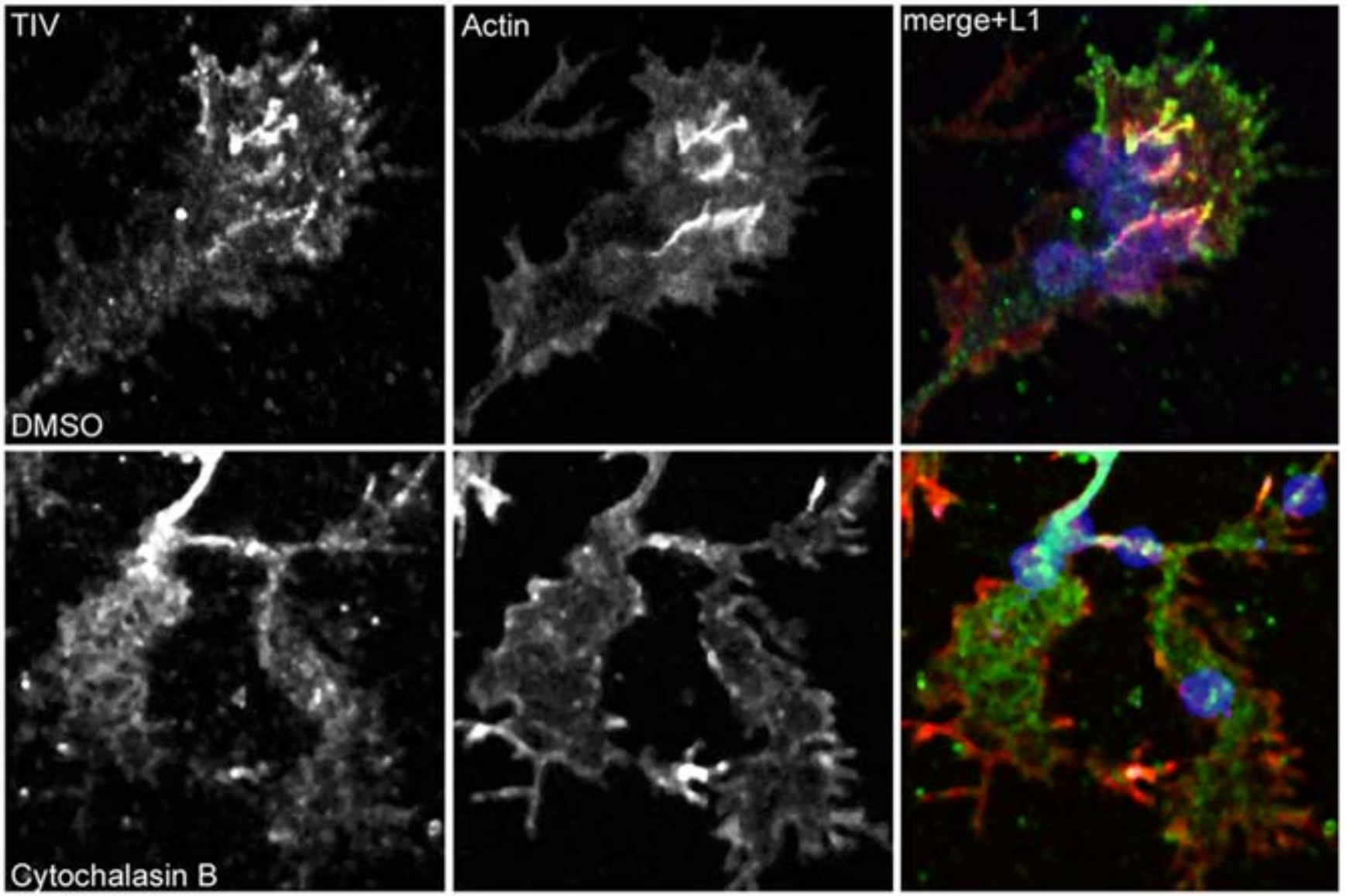
TIV
Actin
merge+L1
DMSO
Cytochalasin B

B)

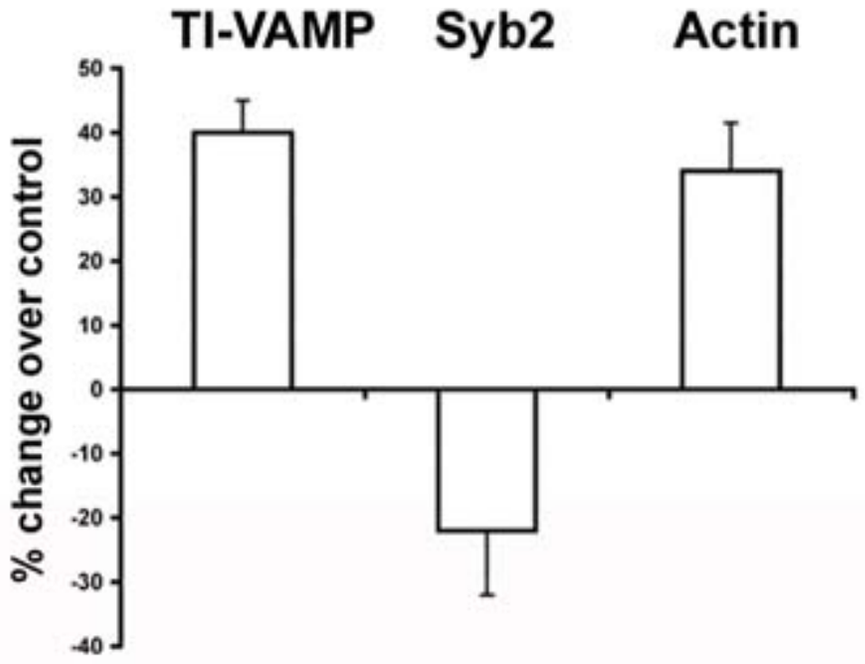
TI-VAMP
Syb2
Actin
% change over control
50
40
30
20
10
0
-10
-20
-30
-40

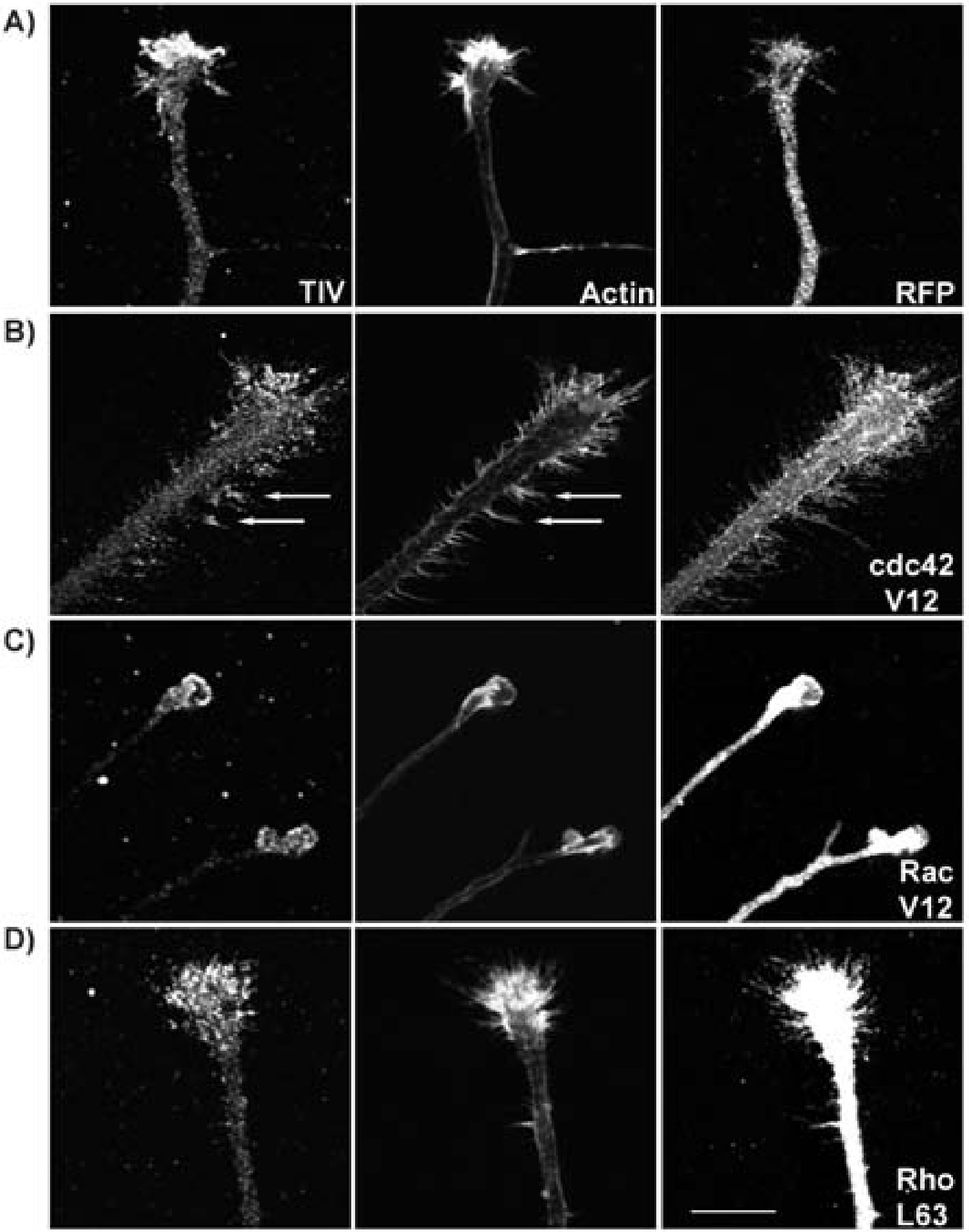
A)
TIV
Actin
RFP
B)
cdc42
V12
C)
Rac
V12
D)
Rho
L63

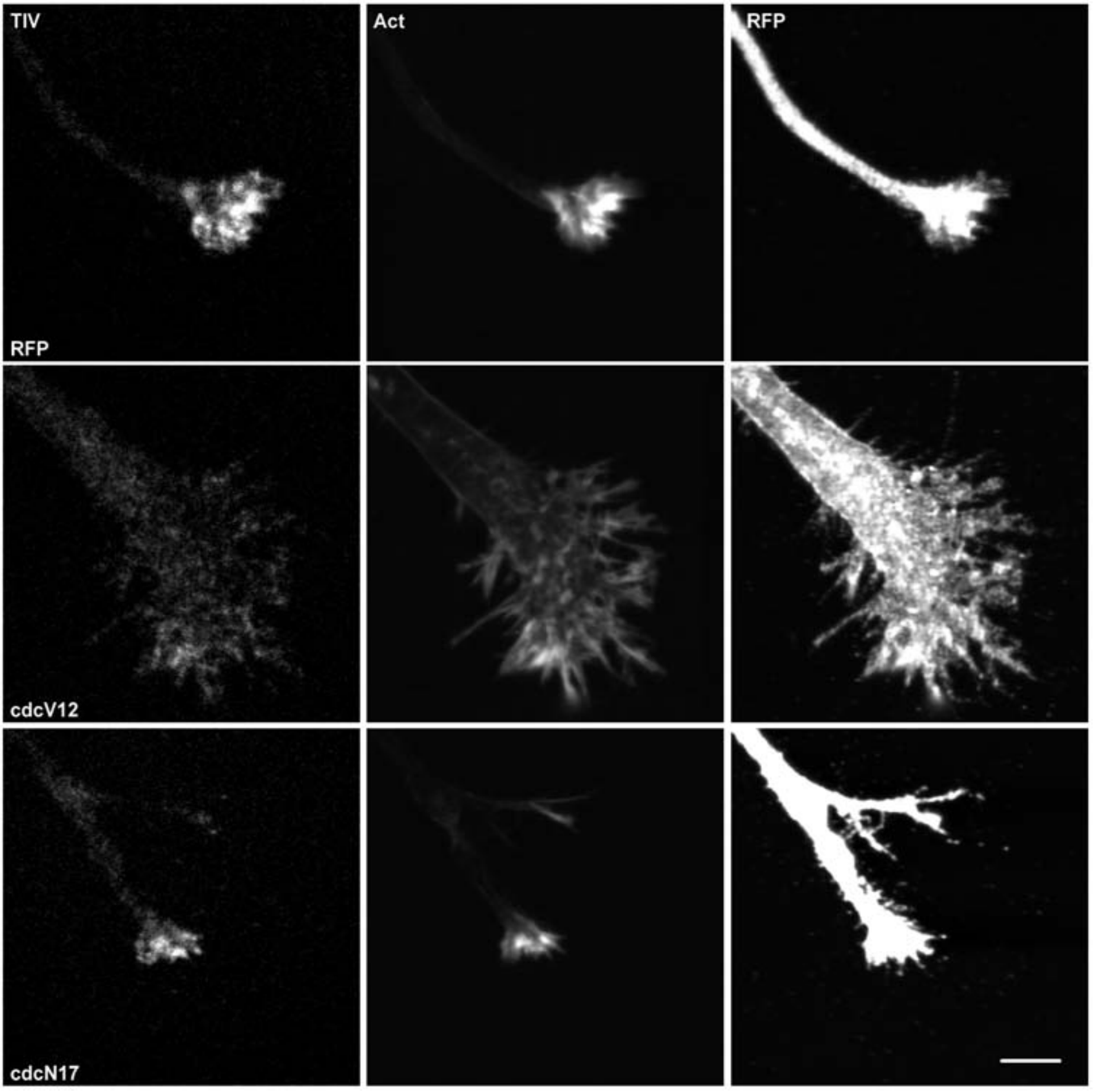
TIV
Act
RFP
RFP
cdcV12
cdcN17

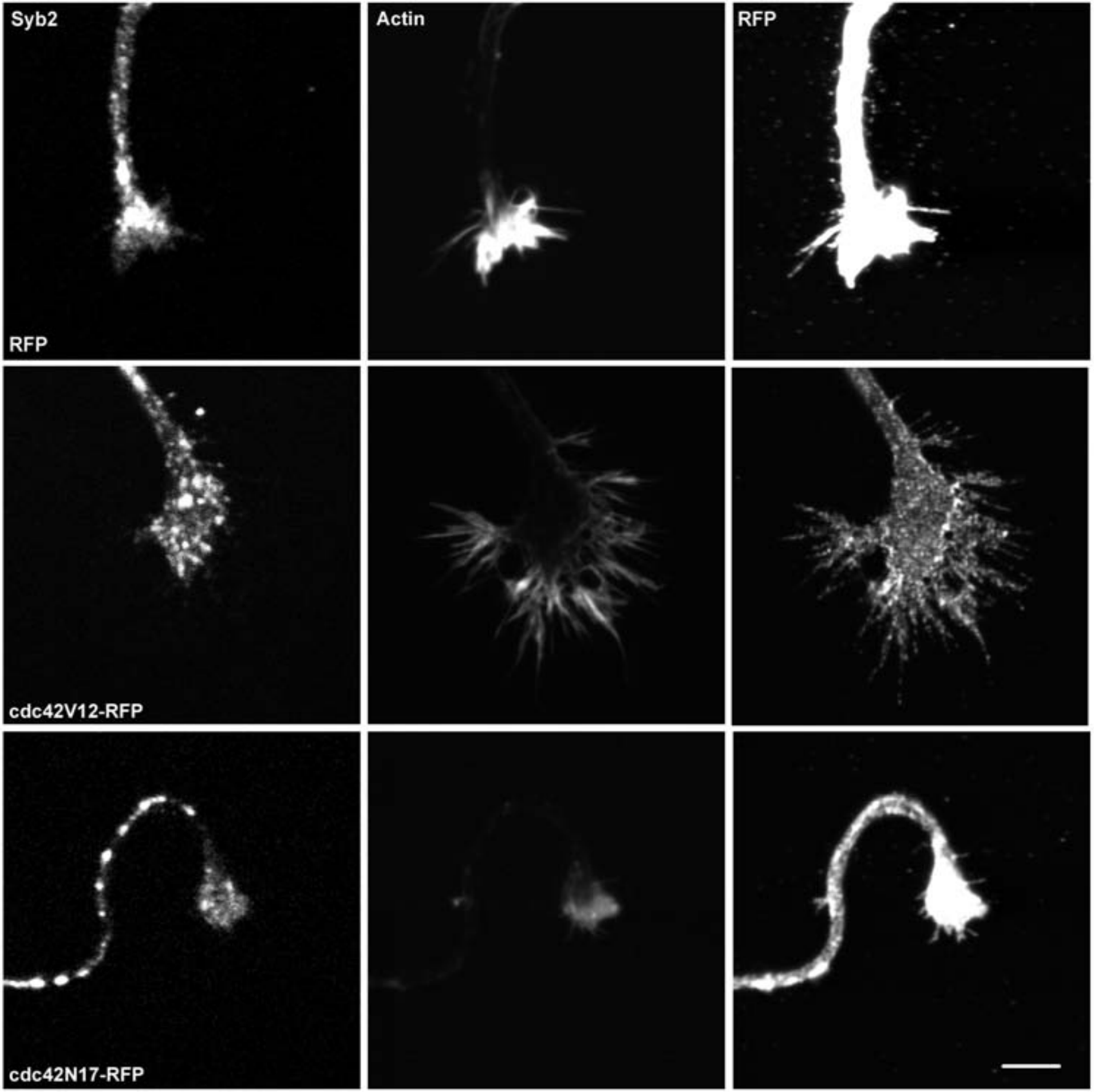
Syb2
Actin
RFP
RFP
cdc42V12-RFP
cdc42N17-RFP

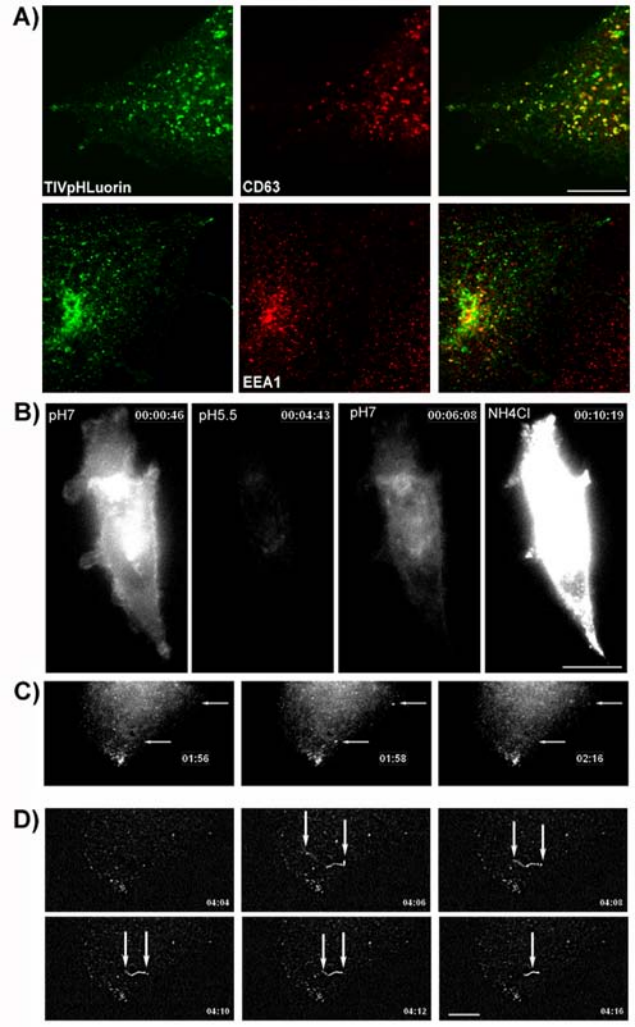
A)
TIVpHLuorin
CD63
EEA1
B)
pH7
00:00:46
pH5.5
00:04:43
pH7
00:06:08
NH4Cl
00:10:19
C)
01:56
01:58
02:16
D)
04:04
04:06
04:08
04:10
04:12
04:16

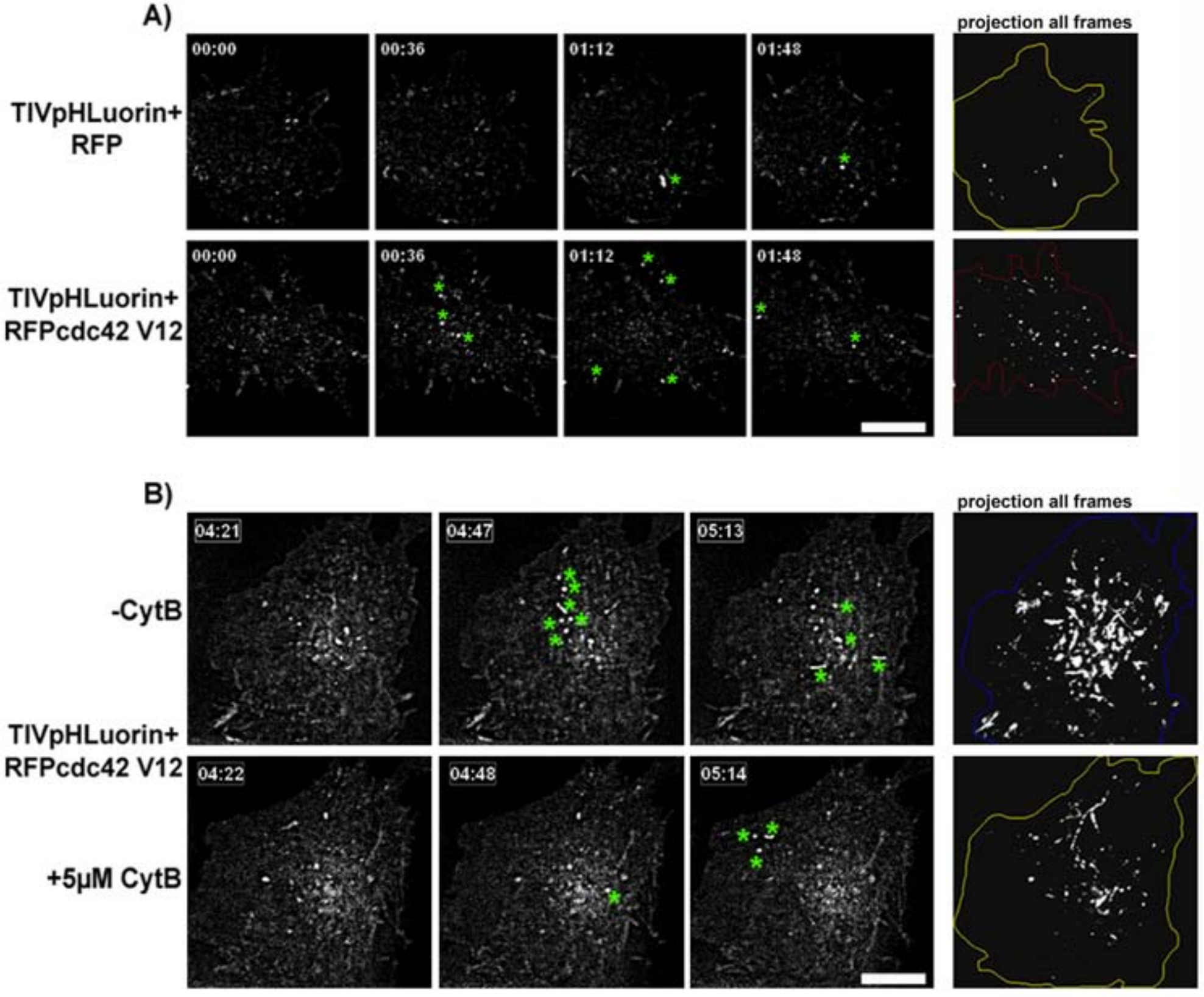
A)
projection all frames
00:00
00:36
01:12
01:48
TIVpHLuorin+
RFP
00:00
00:36
01:12
01:48
TIVpHLuorin+
RFPcdc42 V12
B)
projection all frames
04:21
04:47
05:13
-CytB
TIVpHLuorin+
RFPcdc42 V12
04:22
04:48
05:14
+5µM CytB